Two-Leg Molecular Ladders Formed by Hierarchical Self-Assembly of an Organic Radical

ARTICLE *in* JOURNAL OF THE AMERICAN CHEMICAL SOCIETY · MAY 2009

Impact Factor: 12.11 · DOI: 10.1021/ja900453n · Source: PubMed

14 AUTHORS, INCLUDING:

Andrea Minoia
Université de Mons
30 PUBLICATIONS **435** CITATIONS
SEE PROFILE

Mathieu Linares
Linköping University
63 PUBLICATIONS **983** CITATIONS
SEE PROFILE

Jaume Veciana
Spanish National Research Council
983 PUBLICATIONS **12,403** CITATIONS
SEE PROFILE

Concepcio. Rovira
Spanish National Research Council
528 PUBLICATIONS **9,108** CITATIONS
SEE PROFILE

Article

Two-Leg Molecular Ladders Formed by Hierarchical Self-Assembly of an Organic Radical

Nu#ria Crivillers, Shuhei Furukawa, Andrea Minoia, An Ver Heyen, Marta Mas-Torrent, Christian Sporer, Mathieu Linares, Alexander Volodin, Chris Van Haesendonck, Mark Van der Auweraer, Roberto Lazzaroni, Steven De Feyter, Jaume Veciana, and Concepcio# Rovira

J. Am. Chem. Soc., **2009**, 131 (17), 6246-6252• Publication Date (Web): 10 April 2009

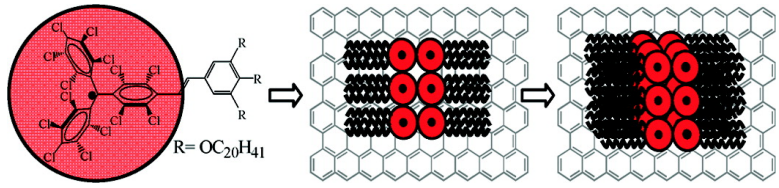

J|A|C|S ARTICLES

Published on Web 04/10/2009

Two-Leg Molecular Ladders Formed by Hierarchical Self-Assembly of an Organic Radical

Núria Crivillers, Shuhei Furukawa,*,† Andrea Minoia, An Ver Heyen, Marta Mas-Torrent, Christian Sporer, Mathieu Linares, Alexander Volodin, Chris Van Haesendonck, Mark Van der Auweraer, Roberto Lazzaroni,* Steven De Feyter,* Jaume Veciana, and Concepció Rovira*

Institut de Ciència de Materials de Barcelona (ICMAB-CSIC), Networking Research Center on Bioengineering, Biomaterials and Nanomedicine (CIBER-BBN), Bellaterra, Spain, Campus Universitari de Bellaterra, 08193 Cerdanyola del Vallès, Spain, Katholieke Universiteit Leuven, Laboratory of Photochemistry and Spectroscopy, and INPAC—Institute for Nanoscale Physics and Chemistry, Celestijnenlaan 200-F, 3001 Heverlee, Belgium, Katholieke Universiteit Leuven, Laboratory of Solid-State Physics and Magnetism, and INPAC—Institute for Nanoscale Physics and Chemistry, Celestijnenlaan 200-D, 3001 Heverlee, Belgium, and Service de Chimie des Matériaux Nouveaux, Université de Mons-Hainaut, 20, Place du Parc, B-7000 Mons, Belgium

Received January 22, 2009; E-mail: shuhei.furukawa@kip.jst.go.jp (S.F.); roberto@averell.umh.ac.be (R.L.); steven.defeyter@chem.kuleuven.be (S.D.F.); cun@icmab.es (C.R.)

Abstract: The supramolecular organization of a new polychlorotriphenyl (PTM) radical bearing three long alkyl chains has been studied by scanning tunneling microscopy (STM) at the liquid−solid interface. This radical hierarchically self-assembles on graphite forming head-to-head dimers that organize in rows following an interesting spin-containing two-leg molecular ladder topology, in which the alkyl chains determine the space between the radical rows and act as diamagnetic barriers. In addition, these double-rows also self-assemble three-dimensionally, leading to a multilayer organization which is still influenced by the HOPG substrate symmetry. The observed nanostructures are sustained by different intermolecular interactions such as Cl···Cl, Cl···Ph, $\pi-\pi$, van der Waals, and CH···π interactions. Theoretical calculations were used to model the observed assemblies, and the results were in complete agreement with the experimental data. Remarkably, atomic force microscopy (AFM) studies confirmed that this tendency to form double rows composed by the PTM magnetic heads surrounded by the alkyl chains is maintained after the complete evaporation of the solvent. The electrochemical and magnetic properties of these PTM nanostructures were also demonstrated.

Introduction

The fabrication of nanometer-scale devices calls for the need to organize functional molecules on a substrate. The use of surface assemblies of stable free organic radicals that are inherently magnetic are interesting for this purpose; however, there are only a few examples in the literature.[1,2] Previously, organic radicals have been deposited on surfaces by vacuum-deposition and drop-casting,[1] and more recently, the preparation of self-assembled monolayers (SAMs) has permitted the formation of bidimensionally organized monolayers of organic radicals chemically bonded to the surface.[2] Polychlorotriphenylmethyl (PTM) radicals are very appealing multifunctional molecules, as in addition to their magnetic properties, these radicals are also optically and electrochemically active and, therefore, are promising building blocks for designing multifunctional molecular materials. PTM radicals are highly stable due to the shielding of the trivalent central carbon atom by the phenyl rings with a propeller-like conformation and the six ortho chlorine atoms.[3] Their high chemical stability has allowed their functionalization to prepare supramolecular materials with a variety of properties, such as porous molecular magnets,[4] systems with nonlinear optical properties,[5] molecular switches in solution,[6] and more recently, switches on surfaces.[2a,b] Interestingly, it was also shown that the magnetic character of the radicals is

† Present address: ERATO Kitagawa Integrated Pores Project, Japan Science and Technology Agency (JST), Kyoto Research Park Bldg 3, Shimogyo-ku, Kyoto 600-8815, Japan.

(1) (a) Durkam, C.; Welland, M. E. *Appl. Phys. Lett.* **2002**, *80*, 458–460. (b) Pong, W.-T.; Durkam, C.; Li, H.; Harneit, W. *J. Scann. Probe Microsc.* **2006**, *1*, 55–62. (c) Guisinger, N. P.; Elder, S. P.; Yolder, N. L.; Hersam, M. C. *Nanotechnology* **2007**, *18*, 1–6. (d) Greene, M. E.; Guisigner, N. P.; Basu, R.; Baluch, A. S.; Hersam, M. C. *Surf. Sci.* **2004**, *559*, 16–28.

(2) (a) Crivillers, N.; Mas-Torrent, M.; Perruchas, S.; Roques, N.; Vidal-Gancedo, J.; Veciana, J.; Rovira, C.; Basabe-Desmonts, L.; Ravoo, B. J.; Crego-Calama, M.; Reinhoudt, D. N. *Angew. Chem., Int. Ed.* **2007**, *46*, 2215–2219. (b) Crivillers, N.; Mas-Torrent, M.; Vidal-Gancedo, J.; Veciana, J.; Rovira, C. *J. Am. Chem. Soc.* **2008**, *130*, 5499–5506. (c) Shekhah, O.; Roques, N.; Mugnaini, V.; Munuera, C.; Ocal, C.; Veciana, J.; Wöll, C. *Langmuir* **2008**, *24*, 6640–6648. (d) Mannini, M.; Sorace, L.; Gorini, L.; Piras, F. M.; Caneschi, A.; Magnani, A.; Menichetti, S.; Gatteschi, D. *Langmuir* **2007**, *23*, 2389–2397. (e) Matsushita, M. M.; Ozaki, N.; Sugawara, T. F.; Nakamura, Hara, M. *Chem. Lett.* **2002**, *6*, 596–597.

(3) (a) Ballester, M.; Riera, J.; Castañer, J.; Badia, C.; Monsó, J. M. *J. Am. Chem. Soc.* **1971**, *93*, 2215–2225. (b) Armet, O.; Veciana, J.; Rovira, C.; Castañer, J.; Molins, E.; Rius, J.; Miravitlles, C.; Olivella, S.; Brichfeus, J. *J. Phys. Chem.* **1987**, *91*, 5608–5616.

 10.1021/ja900453n CCC: $40.75

Scheme 1. Synthesis of PTM Radical **1**

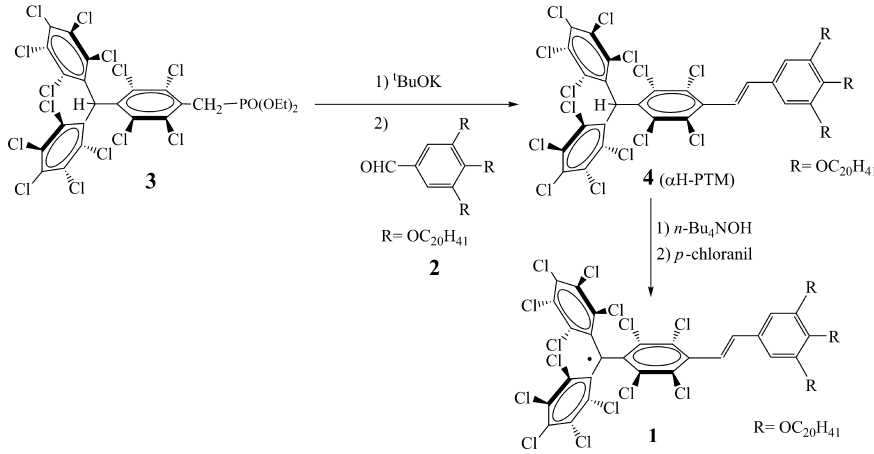

maintained after chemisorption on surfaces.[2a−c] The potential of these materials prompted us to investigate their self-assembly on surfaces by physisorption. In this process, the formation of the molecular assemblies is driven solely by weak intermolecular interactions, that is, the molecules truly self-assemble rather than forcing them to be immobilized on the surface. Here, the novel PTM radical **1** has been investigated physisorbed on graphite at the liquid−solid interface by scanning tunnelling microscopy (STM), since in this environment the molecules can form the thermodynamically most stable supramolecular structures,[7] and in the absence of solvent by atomic force microscopy (AFM). This radical forms well-ordered structures on highly oriented pyrolytic graphite (HOPG) that consist of double rows composed by a magnetic core of radicals surrounded by alkyl chains with a two-leg ladder topology.

Results and Discussion

Taking into account the propeller-like conformation of the PTM moiety and that previous works have shown that in similar bulky systems as C_{60} it is necessary to have more than one long alkyl chain to ensure the adsorption of the molecules on graphite,[8] the derivative **1** bearing three long alkyl chains was synthesized. The protonated PTM precursor **4** (αH-PTM) was prepared by coupling through a Wittig−Horner−Emmons reaction the corresponding alkoxybenzaldehyde[8] and the PTM phosphonate **3**.[9] The αH-PTM **4** was first deprotonated with a base to form the carbanion derivative, which was then oxidized to form the radical **1** in a one-pot reaction (Scheme 1). PTM radical **1** was fully characterized by IR, UV−vis, MALDI-TOF, cyclic voltammetry, and EPR (see Experimental Methods).

The self-assembly of **1** at the liquid−solid interface was investigated by STM in constant current mode and under light exclusion to avoid the decomposition of the radical. A diluted solution (2.5×10^{-4} M) of PTM radical **1** in 1-phenyloctane was applied to a freshly cleaved surface of HOPG. The molecules assembled spontaneously and formed ordered nanostructures at the interface, as illustrated in Figure 1. The bright areas in the STM images were attributed to the bulky and conductive radical PTM moieties. Molecules of radical **1** assemble into characteristic double rows with a peak-to-peak separation of 2.2 ± 0.2 nm (green arrows in Figure 1). The distance between double rows is 8.0 ± 0.2 nm (red arrows in Figure 1), which is in agreement with the size of two extended molecules. It is also worth mentioning that several double rows are aligned in the same direction, forming the so-called domain structures. Interestingly, the observed directions of double rows are restricted only to three directions with an angle close to 120°, which suggests that the molecules interact with HOPG, and therefore, the substrate symmetry strongly affects the growth direction of the rows. Furthermore, each bright line consists of disk-like features 0.8 ± 0.1 nm apart, which might correspond to the PTM cores (Figure 1b). Similar head-to-head organizations have been observed in PTM crystal structures of asymmetric radical derivatives, as **1**, and were attributed to the presence of Cl···Cl interactions.[10]

Surprisingly, one can see less bright double-row structures (blue arrows) in Figure 1. This phenomenon is strongly evidenced in the STM image shown in Figure 2, where double rows are lying over each other forming a multilayer structure. It should be noticed that the double rows from the top layer are still oriented with the angle of 120° with respect to the layer below, which suggests that the symmetry of the HOPG substrate influences the 3-D organization.

This multilayer structure was further confirmed by performing bias-dependent measurements during imaging (Figure 3a). The sample bias applied ranged from −1.5 to −0.2 V. When the bias voltage was −1.5 V, the double rows in the second top layer could be observed. Then, the voltage was increased to −0.5 V (for the same set point current) and only the double row structure from the first bottom-layer was seen. At −0.2 V, no molecules were observed probably because the tip was too close to follow the topography of the molecules and/or because they were removed from the substrate by the tip during the

(4) (a) Maspoch, D.; Ruiz-Molina, D.; Wurst, K.; Domingo, N.; Cavallini, M.; Biscarini, F.; Tejada, J.; Rovira, C.; Veciana, J. *Nat. Mater.* **2003**, *2*, 190–195. (b) Maspoch, D.; Domingo, N.; Ruiz-Molina, D.; Wurst, K.; Tejada, J.; Rovira, C.; Veciana, J. *J. Am. Chem. Soc.* **2004**, *126*, 730–741.
(5) Ratera, I.; Marcen, S.; Montant, S.; Ruiz-Molina, D.; Rovira, C.; Veciana, J.; Létard, J. F-.; Freysz, E. *Chem. Phys. Lett.* **2002**, *363*, 245–251.
(6) (a) Ratera, I.; Ruiz-Molina, D.; Vidal-Gancedo, J.; Wurst, K.; Daro, N.; Létard, J. F.; Rovira, C.; Veciana, J. *Angew. Chem., Int. Ed.* **2001**, *40*, 919–922. (b) Sporer, C.; Ratera, I.; Ruiz-Molina, D.; Zhao, Y.; Vidal-Gancedo, J.; Wurst, K.; Jaitner, P.; Clays, K.; Persoons, A.; Rovira, C.; Veciana, J. *Angew. Chem., Int. Ed.* **2004**, *43*, 5266–5268.
(7) (a) De Feyter, S.; Schryver, F. C. *Chem. Soc. Rev.* **2003**, *32*, 139. (b) Rabe, J.; Buchholz, S. *Science* **1991**, *253*, 424–427.
(8) Nakanishi, T.; Miyashita, N.; Michinobu, T.; Wakayama, Y.; Tsuruoka, T.; Ariga, K.; Kurth, D. G. *J. Am. Chem. Soc.* **2006**, *128*, 6328–6329.
(9) Rovira, C.; Ruiz-Molina, D.; Elsner, O.; Vidal-Gancedo, J.; Bonvoisin, J.; Launay, J.-P.; Veciana, J. *Chem.—Eur. J.* **2001**, *7*, 240–250.
(10) Ribas, X.; Maspoch, D.; Wurst, K.; Veciana, J.; Rovira, C. *Inorg. Chem.* **2006**, *45*, 5383–5392.

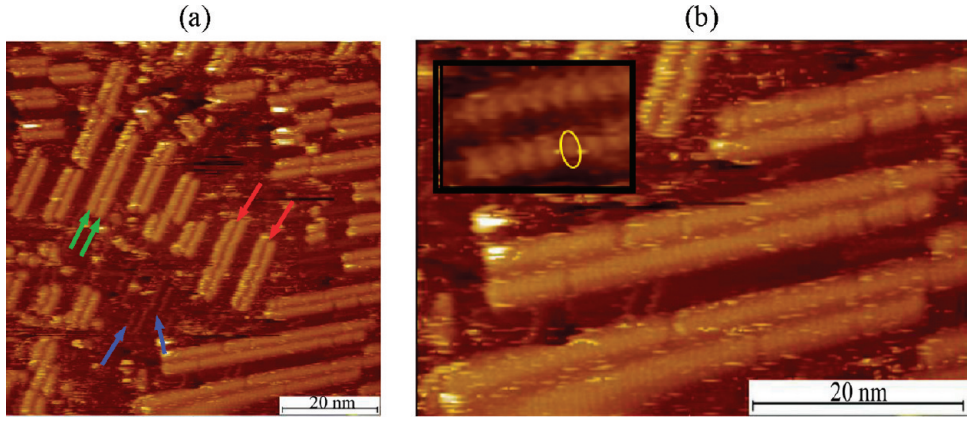

Figure 1. (a) STM image of **1** from 1-phenyloctane on HOPG. $I = 0.023$ nA, $V = -1.0$ V. Green and red arrows indicate the separation between two adjacent rows and between two adjacent double rows, respectively, and blue arrows indicate some double rows from the first bottom layer. (b) Zoom images show the stacked disk-like bright features (highlighted in yellow) which form the rows.

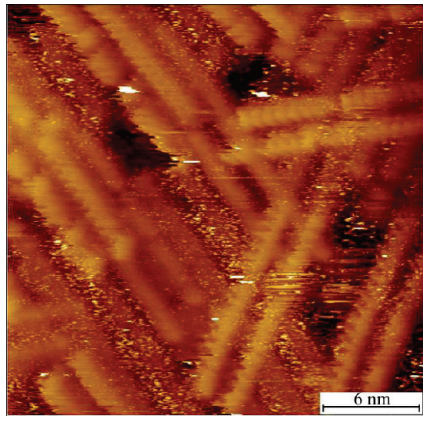

Figure 2. STM image of the multilayer feature of **1**. $I = 0.023$ nA, $V = -1.0$ V.

scanning process. The multilayer formation was also influenced by the solution concentration. Although the multilayer structure was still observed in some areas in a more diluted solution (2.5×10^{-5} M), in many other regions domains with only one monolayer of aligned double rows were found (Figure 3b). The absence of bias voltage dependence in the STM images in these areas is consistent with the presence of only a single molecular layer.

Thus, even though **1** has three long alkyl chains promoting the adsorption of the molecules on HOPG by van der Waals interactions, there is a clear tendency to form a multilayer structure probably due to preferable molecule−molecule interactions. This multilayer structure has previously been observed for other systems mainly promoted by electrostatic or weak S···S interactions.[11−13] In the present case, weak Cl···Cl and/or Cl···Phenyl interactions may be responsible for the multilayer formation which allow to transmit the organizative information vertically from the HOPG to the topmost layers.

In order to better understand the supramolecular organization within the double rows, assemblies of **1** were modeled using an atomistic approach based on force-field molecular mechanics (MM) and molecular dynamics (MD) simulations (see the Supporting Information for more computational details). The first stage of the modeling was dedicated to the analysis of the conformation of the PTM heads and their geometry on the graphite surface. In order to reduce the complexity of the calculations in this first stage, the alkyl chains were replaced by $-CH_3$ groups.[14] The actual alkyl side groups were reintroduced in the second stage, based on the most favorable structures obtained for the PTM heads, to model the assembly of the full molecules on graphite. In all the calculations, the surface was modeled with two "frozen" layers of graphite. Since we were more interested in the equilibrium structure of the supramolecular assemblies than in the process by which they are formed, the presence of the solvent was considered to be of minor importance. This hypothesis is substantiated by the fact that (i) the structures do not evolve in time, i.e., there is no exchange of PTM and solvent molecules between the solution and the surface, and (ii) there is no indication of solvent coadsorption. Therefore, no explicit solvent molecules were introduced in the modeled systems and the solvent was represented as a continuum dielectric medium.

The first step in the modeling of the adsorbate was the identification of the most stable orientations and conformations for a single molecule on the surface. Two conformers were found to be stable: in the first one (A), the two terminal perchlorinated phenyl rings are both interacting with the surface (Figure 4a); in the second one (B), only one of the terminal phenyl rings is in direct contact with the surface and the other one is pointing away from the surface (Figure 4b). Regarding the height of the molecules on the surface, the difference between the two orientations is about 3−4 Å (8−9 and 11−13 Å for the A and B conformation, respectively). Since the topographic profiles extracted from the STM images show that the height is constant along the rows, it is unlikely that those rows contain a mixture of A- and B-type molecules. They are most probably composed of molecules having all the same conformation. On the basis of that, two different models for the double row assembly were considered—the first one, named AA-assembly, is formed by molecules in the A conformation

(11) (a) Stawasz, M. E.; Sampson, D. L.; Parkinson, B. A. *Langmuir* **2000**, *16*, 2326–2346. (b) Stawasz, M. E.; Parkinson, B. A. *Langmuir* **2003**, *19*, 10139–10151.
(12) Lei, S.; Puigmartí-Luis, J.; Minoia, A.; Van der Auweraer, M.; Rovira, C.; Lazzaroni, R.; Amabilino, D. B.; De Feyter, S. *Chem. Commun* **2008**, *70*, 3–705.
(13) Samorı, P.; Severin, N.; Simpson, C. D.; Müllen, K.; Rabe, J. P. *J. Am. Chem. Soc.* **2002**, *124*, 9454.

(14) Control calculations on a small model system have shown that the length of the alkyl group does not affect the conformation of the PTM head.

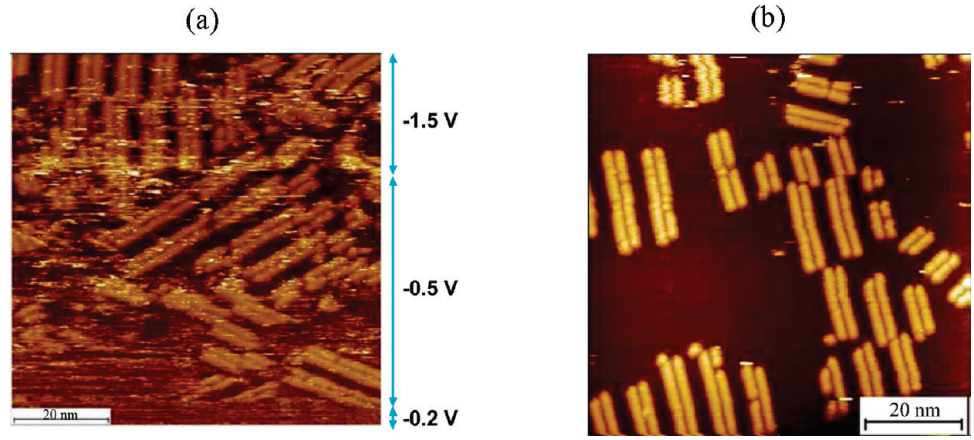

Figure 3. (a) STM image of **1** at different applied bias voltages. $I = 0.023$ nA. (b) STM image of **1** forming a monolayer of aligned double rows. $I = 0.023$ nA, $V = -1.2$ V.

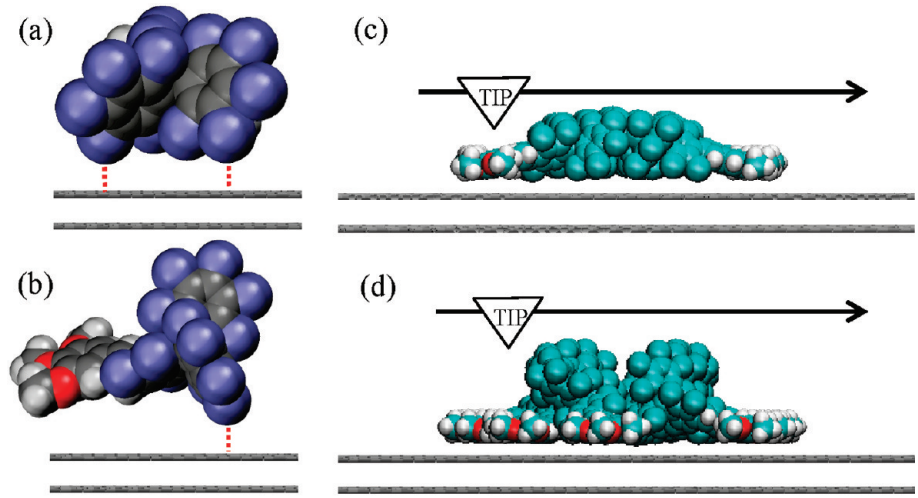

Figure 4. Side views of PTM radical **1** in the molecular conformation (a) A and (b) B (see text). The red dotted lines indicate the closest contacts between the physisorbed molecules and the graphite surface. Side views of the assemblies on graphite: (c) AA and (d) BB.

while the second, named BB-assembly, is formed by molecules in the B orientation (Figure 4c and d). Both models are quite in agreement with the experimental geometry, in terms of the global size of the assembly. In order to discriminate between the two models, the internal energy and the adsorption energy on graphite were calculated with the MM3 force field (see Table 2 in the Supporting Information) for the central part of optimized assemblies of eight molecules. The results show that the two assemblies have roughly the same adsorption energy (within 1.5 kcal/mol), despite the fact that one phenyl ring in the molecules of the BB-assemblies is pointing away from the surface. The difference between the values of the internal energy is also too small to rule out one model.

However, it should be noticed that the STM images clearly show the presence of a dark area between the two rows, which is interpreted as some separation between the molecular rows. The side views of the van der Waals representation of the AA- and BB-assemblies are shown in Figure 4c,d. The side view for the AA-assembly presents a smooth profile along the scan direction, indicated by the black arrow, and thus a single broad feature would be expected in the STM images. In contrast, in the BB-assembly two well-resolved peaks separated by 1.9−2.2 nm along the scan direction should appear, which is in good agreement with the STM profile of 2.2 ± 0.2 nm obtained experimentally. In addition, in the BB-assembly the molecules are slightly closer to each other on average, and this could increase the number of favorable intermolecular interactions through Cl atoms and phenyl groups.

In the second stage, the C20 alkyl chains were introduced in the model and a full MM+MD procedure was carried out. An optimized frame of a long MD trajectory is shown in Figure 5. Due to the dense packing of the PTM heads in the stack, there is not enough space to accommodate all the alkyl chains on the surface, so only two of them are adsorbed on the surface per molecule, while the third one is lying above, as it is shown in the side view (Figure 5 bottom). This is also an indication that there is no space for interdigitation between alkyl chains of adjacent stacks, in agreement with the experimental separation of 8.0 nm observed between adjacent structures in the STM images.

The mean intermolecular distance within a row, obtained from the statistical analysis of the separation between the centers of mass of the heads of adjacent molecules over the MD run, is 0.83 ± 0.06 nm, which fully confirms the interpretation of the inner structure of the rows made from Figure 1b.

Overall, the STM results combined with the molecular modeling point to the fact that **1** hierarchically self-assembles as follows: (1) PTM molecules interact head-to-head giving rise to dimeric structures; (2) the dimers stack, maximizing the van der Waals interactions among adjacent alkyl chains forming the

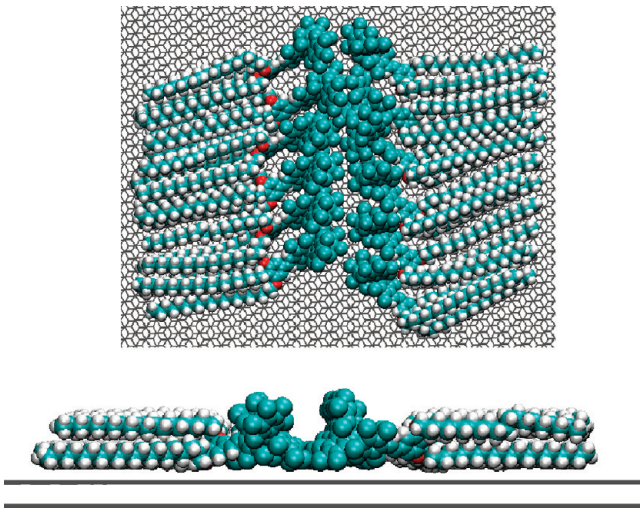

Figure 5. Optimized structure from a snapshot during a MD simulation of the BB-assembly (top and side views). The side view clearly shows the two levels for the alkyl chains.

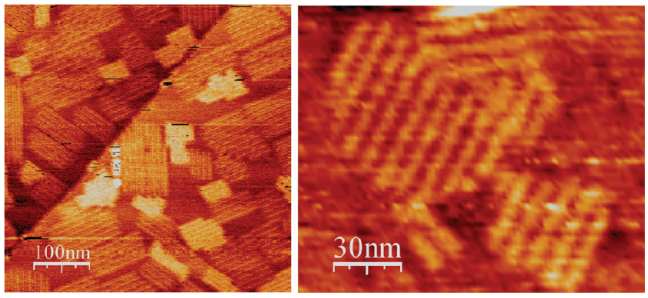

Figure 6. AFM images for a sample prepared from drop-casting a solution of **1** in toluene on HOPG. Left image: Z range 3.5 nm; right image: Z range 1 nm.

double rows which show a two-leg ladder topology; (3) the alkyl chains drive the orientation of the assembled structures on the surfaces via CH$-\pi$ interactions maximizing the commensurability between the alkyl chains and the graphite lattice, and (4) due to molecule−molecule interactions, a layer of double rows lie over the first monolayer, leading to a 3-D multilayer organization, which is still influenced by the HOPG substrate symmetry. Therefore, presumably the self-assembly of **1** on graphite results in the formation of spin-containing two-leg ladders shielded by the alkyl chains that determine the space between the radical rows and act as diamagnetic barriers.

In addition to the STM measurements at the liquid−solid interface, we performed AFM studies on the assemblies that **1** forms in "dry conditions", that is, after complete evaporation of the solvent. The samples were prepared by drop-casting 10 μL of a 2.0×10^{-6} M solution of **1** in toluene on freshly cleaved graphite surfaces and allowing the solvent to evaporate at room temperature. Remarkably, the AFM images demonstrated that radical **1** forms row-like structures over large areas of the substrate (Figure 6). Such one-dimensional structures also follow the symmetry directions of the HOPG substrate. The dimensions of the assemblies are in agreement with the STM results, considering that the bright rows observed in Figure 6 correspond now to the double rows formed by the PTM cores and the dark area in between to the extended alkyl chains. This indicates that radical **1** maintains the molecular organization previously observed in the liquid−solid interface after the solvent evaporation, which is attractive for potential applications.

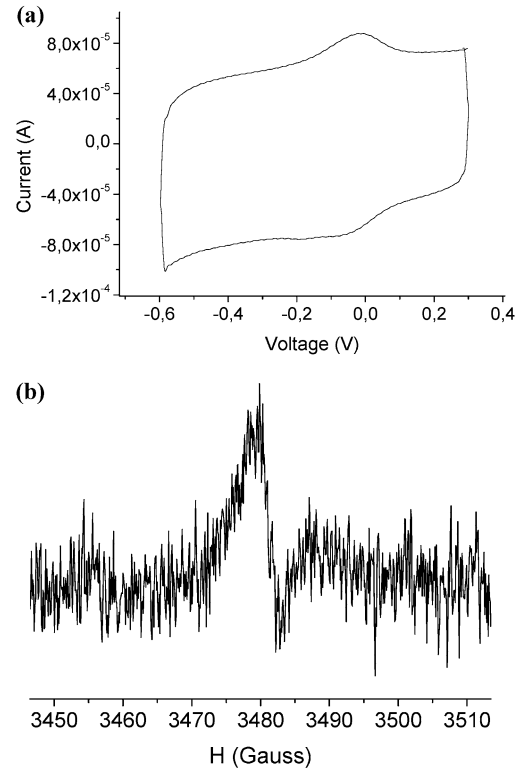

Figure 7. (a) Cyclic voltammogram of **1** on graphite at 1 V/s (experimental conditions: 0.1 M of n-Bu_4NClO_4 in acetonitrile, vs Ag/AgCl). (b) EPR spectrum of **1** on graphite recorded at 300 K.

The electrochemical and magnetic properties of these surface assemblies based on **1** have also been demonstrated. The samples were prepared employing the same conditions as the ones used for the AFM experiments described above. Since the spin-containing assemblies are electroactive, cyclic voltammetry experiments were performed in order to investigate their redox behavior. This was carried out by immersing the HOPG substrate patterned with **1** in a 0.1 M solution of n-Bu_4NClO_4 in dry acetonitrile and employing it as working electrode in a cyclic voltammogram experiment. Figure 7a shows a reversible redox peak at $E_{1/2} = -0.03$ V (vs Ag/AgCl) attributed to the PTM radical−PTM anion redox couple. We also observed that increasing the scan rate resulted in a linear increase in the intensity of the peaks (see Supporting Information), which is characteristic for surface-confined electroactive species. However, for an ideal situation in which electroactive centers are all close to the electrode surface and, therefore, diffusion should not have any influence in the process, and in which the surface attached electroactive groups are noninteracting groups and in rapid equilibrium with the electrode, one would expect no splitting between the oxidation and reduction peaks.[15] In our case, we observed a considerable large separation between the oxidation and reduction potentials ($\Delta E = 30$ mV at 1 V/s). Such peak splitting could be explained by the interaction between the electroactive PTM radicals. One of the parameters that is used to indicate the interaction between redox centers is the full-width at half-maximum of the anodic (or cathodic) voltammetric wave, ΔE_{fwhm}. In the ideal situation, where there is no interaction between the redox centers, $\Delta E_{fwhm} = 3.53RT/nF$

(15) Murray, R. W.; In *Electroanalytical Chemical Vol.* 13; Bard, A. J., Ed.; Marcel Dekker: New York, 1984; pp 191−368 and references therein.

(90.6 mV/n at 25 °C), n being the number of electrons transferred in the process.[16] The deviations from this value have been attributed to the interaction between the redox centers. In the case of the surface assemblies of PTM **1**, the ΔE_{fwhm} is 187 mV at a scan rate of 1 V/s and, hence, reinforces the idea that there are significant interactions between the spin-containing PTM moieties due to their specific ladder organization on the surface. It cannot be ruled out though that the peak separation is also influenced by the diffusion of the electrolyte into the multilayer structure.

The magnetic characteristics were studied by electron paramagnetic resonance (EPR). The EPR spectrum recorded at 300 K showed a signal with a g value and a line width of 2.0028 and 4.1 G, respectively, which is in accordance with the ones previously reported for a PTM radical SAM (Figure 7b).[2a−c] In fact, the observed g value is the same as the one found for radical **1** in solution, whereas the line width is larger than that obtained in solution due to the fact that the molecules are now immobilized on a surface. Thus, these results clearly prove that the radical character of **1** is preserved on the graphite substrate leading to multifunctional surfaces.

Moreover, the 3-D self-assembly of **1** was also investigated using more concentrated solutions. In this case, the samples were prepared by drop-casting 30 μL of a 2.0×10^{-4} M solution of **1** in toluene. Bundles of individual fibers with a distance (center-to-center) between the rows of the order of 8 nm were observed, in accordance with the STM experiments (see Supporting Information). It is also worth mentioning that, similar to previous experiments, these aggregates were also aligned in three well-defined directions confirming that the symmetry of the HOPG also influences the molecular assemblies under these conditions. These studies reveal that radical **1** has also a strong tendency to form supramolecular 1-D organizations forming fibrilar structures at the micrometer scale, as previously observed with similar systems.[17]

Conclusion

In conclusion, self-assembly is a promising tool for constructing functional supramolecular architectures with an unpaired spin in the repetitive unit. We presented the organization of a novel organic radical derivative that hierarchically self-assembles giving rise to 3-D nanostructures sustained by intermolecular interactions of different nature, such as Cl···Cl, Cl···Ph, $\pi\cdots\pi$, van der Waals, and CH$\cdots\pi$ interactions between alkyl chains and the graphite substrate. The long alkyl chains have two main effects on the reported system: first, they help to obtain well-ordered spin-containing two-leg ladder with a specific space between them, and second, they act as diamagnetic barriers between neighboring radical rows, the magnetic and electrical properties of which have also been proved. The fabrication of ordered nanostructures of interacting organic radicals that form promising topologies like a two-leg spin ladder[18] represents an important step forward in the field of molecular electronics and molecular magnetism for which important physical properties are foreseen.

Experimental Methods

STM. All experiments were performed at 20−22 °C and were performed using a PicoSPM (Molecular Imaging, Tempe, AZ). Pt/Ir STM tips were prepared by mechanical cutting. 1-phenyloctane was purchased by Aldrich. HOPG (grade ZTB) used was from Advanced Ceramics Inc., Cleveland, OH. The bias voltage was applied to the sample in such a way that at negative bias voltage, electrons tunnel from the sample to the tip. The median filter (3 × 3) was applied to all STM images in order to remove the sharp noises.

AFM. The image in Figure 6 (left) was recorded with a commercial scanning force microscope PicoSPM, Agilent 4500 SPM from Molecular Imaging operating in intermittent contact mode and in air at room temperature. We used a silicon tip from Nanosensors with a $K \approx 40$ N/m and a resonance frequency of ∼60 KHz. The image in Figure 6 (right) was recorded with a Multimode microscope from Digital Instruments (Veeco), using a ultrasharp silicon tip with a $K = 0.65$ N/m and a resonance frequency of ∼45 KHz.

EPR spectra were obtained at room temperature using a Bruker ELEXYS E500 X-band spectrometer. A rectangular TE102 cavity was used for the measurements. The signal-to-noise ratio of spectra was increased by accumulation of scans using the F/F lock accessory to guarantee large field reproducibility. Precautions to avoid undesirable spectral distortions and line broadenings, such as those arising from microwave power saturation and magnetic field over modulation, were also taken into account. In these conditions EPR spectrum of an HOPG sheet was recorded and used as a reference. For the acquisition of the EPR spectra of **1** on HOPG, 20 μL of a 2×10^{-6} M solution in toluene were drop-cast on the substrate used as a reference, and the solvent was let to evaporate under ambient conditions. The EPR signal from **1** was obtained after subtraction of the signal coming from the substrate.

Electrochemical experiments in solution were performed with a Potensiostat/Galvanostat VersaSTAT 3 from Princeton Applied Research, by using platinum wires as working and counter electrode, an Ag/AgCl electrode as reference electrode and a solution of 0.1 M of tetrabutylammonium hexafluorophosphate in anhydrous CH_2Cl_2 as supporting electrolyte. Cyclic voltammetry experiments on HOPG substrate were performed using the HOPG substrate as working electrode and a 0.1 M solution of tetrabutylammonium perchlorate in dry acetonitrile as supporting electrolyte. The samples were prepared by drop-casting 20 μL of a 2×10^{-6} M solution of **1** in toluene on both sides of the HOPG substrate and allowing the solvent to evaporate.

Theoretical Calculations. Force-field-based calculations have been used to model the stability on the surface, first for a single molecule, then for stacks of molecules. Control calculations on a small model system have shown that the length of the alkyl group does not affect the conformation of the PTM head. We used the molecular modeling package TINKER 4.2 with the MM3(2000) force field, which has been recently reparameterized to give a better description of weak interactions such as $\pi-\pi$ stacking and CH$-\pi$ interactions. All the MD simulations have been performed in the canonical ensemble (constant NVT) at room temperature, during 200 ps after equilibrating the system. We used periodic boundary conditions to perform calculations on infinite adsorbed layers, with molecules assembled on a two-layer-thick slab of graphite. The graphite layers have been frozen during the simulations since the physisorption of molecules is not expected to affect the structure of the substrate (see the Supporting Information for more computational details).

Synthesis and Characterization. Compounds 2 and 3 (refs 8, 19). The synthesis was carried out as previously described in the literature and **2** and **3** were satisfactory characterized.

Compound 4. Under dry conditions, 23.7 mg (0.21 mmol) of potassium-*tert*-butoxide was added to a solution of phosponate **3** (120 mg, 0.14 mmol) in 4 mL of dry THF at −78 °C.[19] The resulting yellow-orange ylide solution was stirred for 15 min, and then the temperature was increased to 0 °C with an ice bath. Then, a suspension of 152 mg (0.15 mmol) of aldehyde **2** in dry THF

(16) Bard, A. J.; Faulkner, L. R. *Electrochemical Methods: Fundamentals and Applications*; John Wiley and Sons: New York, 1980; p 522.
(17) Nakanishi, T.; Schmitt, W.; Michinobu, T.; Kurth, D. G.; Ariga, K. *Chem.Commun.* **2005**, 5982–5984.

was added slowly. The resulting mixture was stirred for 48 h and then finally quenched by addition of 5 mL of HCl (1 N). The crude product was extracted with $CHCl_3$ (4 × 25 mL), and the organic layer was washed with water (25 mL), dried with Na_2SO_4, and filtered. The solvent was evaporated under reduced pressure. Chromatographic purification with silica gel (hexane/CH_2Cl_2, 2/1) yielded compound **4** (85 mg, 33%). ^{1}H NMR (600 MHz, $CDCl_3$): δ 7.02 (s, 1H, αH), 6.97 (d, J = 16.1 Hz, 1H, −C6Cl4−C*H*−CH−), 6.91 (d, J = 16.1 Hz, 1H, $-C_6C_{l4}-CH-CH-$), 6.72 (s, 2H, ArH), 4.02 (t, J = 6.3 Hz, 4H, $-O-CH_2-$), 3.98 (t, J = 6.3 Hz, 2H, $-O-CH_2-$), 1.79 (m, 6H, $-CH_2-$), 1.54−1,26 (m, 102H, $-CH_2-$), 0.88 (t, J = 6.3 Hz, 9H, $-CH_3$); FT-IR (KBr) ν_{max}: 2918 (s), 2850 (s), 1467 (w), 1374 (w), 1337 (w), 1239 (w), 1119 (w), 873 (w), 809 (w), 776 (w), 721 cm^{-1} (w); MALDI-TOF (negative mode): ($C_{87}Cl_{l4}H_{128}O_3$, M: 1718.3); (*m*/*z*) [M − 2]$^-$=1716.1; [M − 2 − 70(2Cl)]$^-$ = 1646; [M − 2 − 105(3Cl)]$^-$ = 1612.

Compound 1. In absence of light, an aqueous solution of tetra-*n*-butyl ammonium hydroxide (17 μL, 0.026 mmol) was added to a solution of compound **4** (25.3 mg, 14.5 mmol) in 1 mL of dry tetrahydrofurane at room temperature. The red-purple solution was stirred for 1 h. Then, 20.6 mg (0.084 mmol) of *p*-chloranyl was added. The mixture was stirred for 6 h. Then, the solvent was evaporated under vacuum, and the obtained crude was purified by column chromatography (silica gel, $CHCl_3$/hexane, 1/1). A green crystalline compound was obtained (23 mg, 92%). IR (KBr) ν_{max}: 2918 (s), 2850 (s), 1578 (w), 1501 (w), 1467 (m), 1432 (w), 1336 (m), 1262 (w), 1118 (w), 815 (w), 719 cm^{-1} (w); MALDI-TOF (negative mode): ($C_{87}Cl_{l4}H_{127}O_3$, M: 1717.3); (*m*/*z*) [M − 1]$^-$=1716.2, [M − 1 − 70(2Cl)]$^-$ = 1646, [M − 1 − 70 (2Cl) − 225($(CH_2)_{15}CH_3$)]$^-$ = 1421; UV−vis (THF): $\lambda_{max}(\varepsilon)$ = 385 (28 405), 455 (6826), 649 nm (1536); electrochemistry [CH_2Cl_2, vs Ag/ACl]: $E_{1/2,PTM(rad)/PTM(anion)} = -0.172$ V and $E_{ox,ring} = 1.148$ V; EPR (in CH_2Cl_2): g = 2.0026; a (^{1}H) = 2.1 G; a ($^{13}C_\alpha$) = 30.3 G; a ($^{13}C_{arom}$) = 9.2 i 14.2 G; ΔH_{pp} = 1.3 G at 300 K.

Acknowledgment. This work was funded by the EC FP7 ONE-P large-scale project, the Marie Curie RTN CHEXTAN (MRTN-CT-2004-512161) project, the EC FP6 Magmanet NoE (Contract No. 515767-2), funds from the Belgian Federal Science Policy Office through IAP-6/27, FNRS-Belgium, the DGI, Spain (Project No. EMOCIONa, CTQ2006-06333/BQU) and the Instituto Carlos III, MSyC, through "Acciones CIBER". S.F. is grateful to the JSPS Postdoctoral Fellowship for Research Abroad, and N.C. thanks the Ministerio de Ciencia y Tecnología for a Ph.D. fellowship.

Supporting Information Available: Additional AFM images, EPR and electrochemical data, and computational details (including the energies and Cartesian coordinates for the systems described in Figures 4c,d and 5). This material is available free of charge via the Internet at http://pubs.acs.org.

JA900453N

(18) (a) Shapiro, A.; Landee, C. P.; Turnbull, M. M.; Jornet, J.; Deumal, M.; Novoa, J. J.; Robb, M. A.; Lewis, W. *J. Am. Chem. Soc.* **2007**, *129*, 952–959. (b) Rovira, C. *Chem. -Eur. J.,* **2000**, *6*, 1723–1729. (c) Ribas, X.; Mas-Torrent, M.; Pérez-Benítez, A.; Dias, J. C.; Alves, H.; Lopes, E. B.; Henriques, R. T.; Molins, E.; Santos, I. C.; Wurst, K.; Foury-Leylekian, P.; Almeida, M.; Veciana, J.; Rovira, C. *Adv. Funct. Mater.* **2005**, *15*, 1023–1035.

(19) Rovira, C.; Ruiz-Molina, D.; Elsner, O.; Vidal-Gancedo, J.; Bonvoisin, J.; Launay, J.-P.; Veciana, J. *Chem.—Eur. J.* **2001**, *7*, 240–250.